Proc. Int. Conf. Strongly Correlated Electron Systems (SCES2019)
JPS Conf. Proc. **30**, 011120 (2020)
https://doi.org/10.7566/JPSCP.30.011120

Optical Conductivity Study of f Electron States in $YbCu_2Ge_2$ at High Pressures to 20 GPa

Hidekazu Okamura[1], Makoto Nagata[2], Atsushi Tsubouchi[1], Yoshichika Ōnuki[3], Yuka Ikemoto[4], and Taro Moriwaki[4]

[1] *Graduate School of Advanced Technology and Science, Tokushima University, Tokushima 770-8506, Japan*
[2] *Graduate School of Science, Kobe University, Kobe 657-8501, Japan*
[3] *Faculty of Science, University of the Ryukyus, Okinawa 903-0213, Japan*
[4] *Japan Synchrotron Radiation Research Center, Hyogo 679-5198, Japan*

E-mail: ho@tokushima-u.ac.jp

(Received September 10, 2019)

Optical conductivity [$\sigma(\omega)$] of $YbCu_2Ge_2$ has been measured at external pressures (P) to 20 GPa, to study the P evolution of f electron hybridized states. At P=0, $\sigma(\omega)$ shows a marked mid-infrared (mIR) peak at 0.37 eV, which is due to optical excitations from f^{14} (Yb^{2+}) state located below the Fermi level. With increasing P, the mIR peak shows significant shifts to lower energy, reaching 0.18 eV at P=20 GPa. This result indicates that the f^{14} energy level increases toward the Fermi level with P. Such a shift of the f electron level with P has been expected from theoretical considerations, but had never been demonstrated by spectroscopic experiment under high P. The obtained results are also analyzed in terms of the P evolution of the conduction-f electron hybridization.

KEYWORDS: f electron hybridized state, high pressure, optical conductivity

1. Introduction

Duality between localized and delocalized characteristics exhibited by the f electrons has been a central issue in the physics of heavy fermion (HF) compounds, which are typically Ce- or Yb-containing metals. Since the f orbitals are much more localized near the nucleus than the conduction (c) electron states, the f electrons intrinsically have localized characteristics. However, they may become partly delocalized through a hybridization with the c electrons. The degree of localization/delocalization depends on the strength of the hybridization. Strongly localized (weakly hybridized) f electrons lead to interesting phenomena such as effective mass (m^*) enhancement and magnetic order at low temperatures (T). On the other hand, strongly delocalized (strongly hybridized) f electrons lead to intermediate valence (IV) states, where the average Ce (Yb) valence takes a non-integer value between 3 and 4 (2 and 3). The delocalized systems, in particular Yb-based IV compounds, are also quite interesting since their electronic states can be tuned by external pressure (P) over a wide range from delocalized to localized ones. Since an Yb^{3+} has a smaller ionic radius than an Yb^{2+}, an external P generally drives an IV Yb compound toward Yb^{3+} state. $YbCu_2Ge_2$ [1–4] is a good example of such Yb compounds: At P=0, $YbCu_2Ge_2$ shows a Pauli paramagnetism, with a specific heat coefficient (γ) of 10 mJ/K^{2}mol, and Yb is expected to be almost divalent [1]. With increasing P, however, the Yb valence increases [2], and A, the T^2 coefficient of resistivity $\rho(T)$, also increases significantly, indicating a large enhancement in m^* [3]. These results show that the f electron states are strongly affected by P, and that

they become more localized at high P.

To study the microscopic c-f hybridized states, the optical conductivity [$\sigma(\omega)$] technique has played important roles [5]. Typically, $\sigma(\omega)$ of a Ce or Yb HF compound shows a marked mid-infrared (mIR) peak, which has been discussed in terms of the c-f hybridized states near the Fermi level ($E_{\rm F}$). In particular, a universal relation regarding the mIR peak has been found, namely, the mid-IR peak energy ($E_{\rm mIR}$) is roughly proportional to the c-f hybridization energy over many Ce and Yb HF compounds [6]. Therefore, $\sigma(\omega)$ study under high P is expected to be a useful probe for the electronic states in $YbCu_2Ge_2$ at high P. In this work, we have measured $\sigma(\omega)$ of $YbCu_2Ge_2$ at high P to 20 GPa.

2. Experimental

The samples of $YbCu_2Ge_2$ used were single crystals grown with self-flux method [1]. The optical reflectance spectra at high P were measured using a diamond anvil cell (DAC) [7]. Type IIa diamond anvils with 0.8 and 0.6 mm culet diameter and a stainless steel gasket were used to seal the sample with NaCl as the pressure transmitting medium. A flat, as-grown surface of a sample was directly attached on the culet surface of the diamond anvil, and the reflectance at the sample/diamond interface, denoted as $R_d(\omega)$, was measured. A gold film was placed between the gasket and anvil as a reference of $R_d(\omega)$. Small ruby pieces were also sealed to monitor the pressure via its fluorescence. A part of the measurements was made with synchrotron radiation as a bright IR source [8] at the beamline BL43IR of SPring-8 [9, 10]. $\sigma(\omega)$ was derived from $R_d(\omega)$ using the Kramres-Kronig (KK) analysis [11]. In the KK analysis of $R_d(\omega)$, the refractive index of diamond (n_d=2.4) was taken into account as previously described [12]. Below the measured energy range, $R_d(\omega)$ was extrapolated with the Hagen-Rubens function [11]. More details of the high pressure IR experiments can be found elsewhere [7].

3. Results and Discussions

Figure 1(a) shows $R_d(\omega)$ of $YbCu_2Ge_2$ measured with DAC at 295 K and at high P to 20 GPa. The thick, solid curves indicate the original reflectance data, but the data in the range 0.24-0.3 eV are not indicated. This is because this range could not be measured well due to strong absorption by the diamond. To complete the spectra, therefore, they were smoothly interpolated as indicated by the thin solid curves in Fig. 1(a), and the interpolated spectra alone are again shown in Fig. 1(b). It is clear that $R_d(\omega)$ of $YbCu_2Ge_2$ has significant P dependences over the entire measured spectral range. At 2 GPa, $R_d(\omega)$ has a deep minimum centered near 0.27 eV, then it gradually decreases with increasing photon energy. In the deep minimum portion below 0.5 eV, with increasing P, $R_d(\omega)$ increases and the minimum becomes shallower and shifts to lower photon energy. These P evolutions occur much more rapidly above 10 GPa than below 10 GPa. At the same time, in the spectral range above 0.9 eV, $R_d(\omega)$ decreases with P. In contrast to the P evolution below 0.5 eV discussed above, that above 0.9 eV is much more rapid below 10 GPa than above 10 GPa.

Figure 1(c) shows $\sigma(\omega)$ spectra of $YbCu_2Ge_2$ at high P, obtained from the $R_d(\omega)$ spectra in Fig. 1(b) using the KK analysis. The main feature in $\sigma(\omega)$ is a pronounced mIR peak, which progressively shifts to lower energy with P, from 0.36 eV at P=2 GPa to 0.18 eV at P=20 GPa. As a check for the KK analysis, the $\sigma(0)$ values at 2 and 20 GPa, taken from the $\rho(T)$ study [3], are also displayed by the two dots in Fig. 1(c). As shown by the broken curves, the obtained $\sigma(\omega)$ connect reasonably with $\sigma(0)$, indicating the appropriateness of the KK analysis despite the lack of $R_d(\omega)$ data in the far IR range. As mentioned in Introduction,

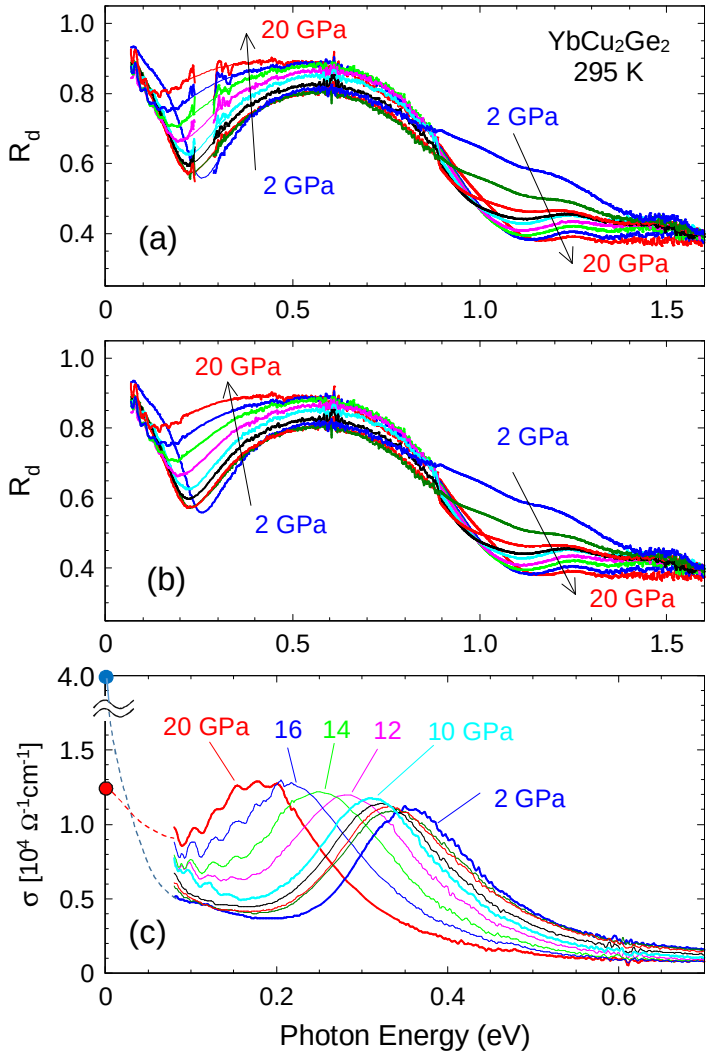

Fig. 1. (a)Reflectance spectra (R_d) of $YbCu_2Ge_2$ measured with DAC at 295 K and at P=2, 4, 6, 8, 10, 12, 14, 16, and 20 GPa. The thick solid curves show the original data, where a spectral range around 0.27 eV is not indicated since this range could not be measured well due to strong absorption by the diamond. The thin solid curves show the interpolations, which smoothly connect the spectra at both sides of the diamond absorption range. (b) The interpolated R_d spectra alone are shown. (c) Optical conductivity (σ) spectra of $YbCu_2Ge_2$ at high P obtained by the Kramers-Kronig analysis of the reflectance spectra in (b). The two dots on the vertical axis indicate the dc conductivities at 2 GPa (blue) and 20 GPa (red) from Ref. [3] and the broken curves are guide to the eye.

many previous studies on Yb-based HF compounds found similar mIR peaks. However, the present result is remarkable in that the mIR peak is so well-separated from the Drude (free carrier) component peaked at zero energy. [Note that a Drude component is not seen in Fig. 1(c) since it is located at lower photon energies below our measurement range, as suggested by the broken curves.] As already mentioned, it has been found that the peak energy $E_{\rm mIR}$ is roughly proportional to the c-f hybridization energy ($\widetilde{V}$) over many compounds with different values of $\widetilde{V}$ [6]. The hybridization is expected to be strongly P dependent, so it is interesting to analyze the P evolution of $E_{\rm mIR}$ in terms of $\widetilde{V}$. Although γ data was used to estimate $\widetilde{V}$ in the previous study [6], γ of $YbCu_2Ge_2$ at high P is unavailable. However, A

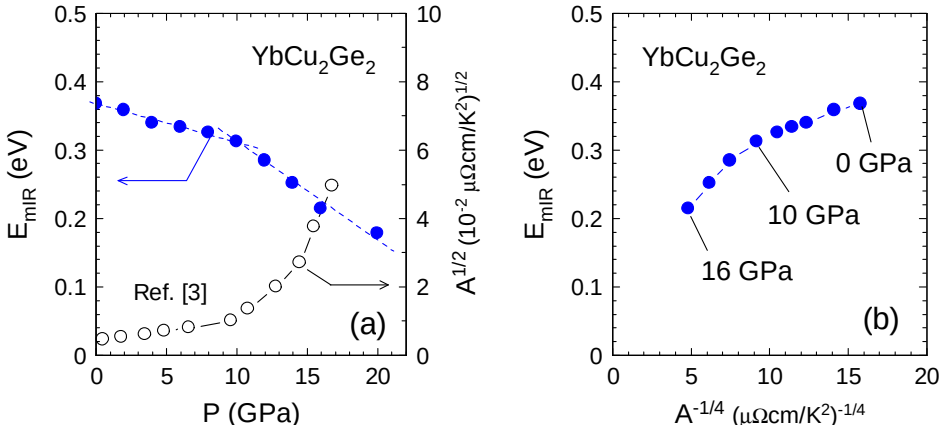

Fig. 2. (a)Measured peak energy ($E_{\rm mIR}$) of the mIR peak in $\sigma(\omega)$ and the $A^{1/2}$ data taken from Miyake *et al.* [3] plotted as a function of pressure (P). The broken lines are guide to the eye, emphasizing the different P dependences of $E_{\rm mIR}$ below and above 10 GPa. (b) $E_{\rm mIR}$ plotted as a function of $A^{-1/4}$. Here, $A^{-1/4}$ is proportional to $\sqrt{T_{\rm K}}$, which in turn is proportional to the renormalized hybridization energy $\widetilde{V}$. Hence, this graph effectively compares $E_{\rm mIR}$ with $\widetilde{V}$.

data of $YbCu_2Ge_2$ at high P are available [3]. Since $A^{1/2}$ is proportional to m^*, it is inversely proportional to the Kondo temperature $T_{\rm K}$. The hybridization is expressed as $2\widetilde{V} \simeq \sqrt{WT_{\rm K}}$ [13, 14], where W is the bandwidth of the c band. Therefore, if W does not change with P, we have $\widetilde{V} \propto A^{-1/4}$, and we may utilize the $A^{1/2}$ data to analyze the evolution of $E_{\rm mIR}$ in terms of $\widetilde{V}$.

Figure 2(a) compares the measured P evolution of $E_{\rm mIR}$ with that of the reported $A^{1/2}$ data [3]. [$\sigma(\omega)$ at P=0 was measured without DAC, but not shown here.] Note that the decrease of $E_{\rm mIR}$ with P is not monotonic, but that above 10 GPa is more rapid than that below 10 GPa as emphasized by the broken lines in Fig. 2(a). A similar tendency is also seen for the $A^{1/2}$ data, namely the increase of $A^{1/2}$ above 10 GPa is more rapid than that below 10 GPa, indicating that m^* increases with P more rapidly above 10 GPa. Namely, both $E_{\rm mIR}$ and m^* vary with P more rapidly above 10 GPa. Although $\sigma(\omega)$ was measured at 295 K and $A^{1/2}$ at much lower T, it seems likely that these results of $E_{\rm mIR}$ and $A^{1/2}$ are related to each other. Figure 2(b) shows plots of $E_{\rm mIR}$ as a function of $A^{-1/4}$. As discussed above, $\widetilde{V} \propto A^{-1/4}$ if W is independent of P. Hence, Fig. 2(b) is effectively a graph of $E_{\rm mIR}$ as a function of $\widetilde{V}$. In the c-f hybridized band model, $E_{\rm mIR} \simeq 2\widetilde{V}$, and if this model is applied here, $E_{\rm mIR} \propto A^{-1/4}$ is expected. However, this is apparently not the case in Fig. 2(b), where $E_{\rm mIR}$ is not quite proportional to $A^{-1/4}$. Nevertheless, $E_{\rm mIR}$ is indeed an increasing function of $A^{-1/4}$, and the move of the plot to lower left with P is consistent with a decrease of $\widetilde{V}$ expected from the observed increase of $A^{1/2}$ at high P. When the ($E_{\rm mIR}$-$A^{-1/4}$) relation of Fig. 2(b) is plotted in the universal ($E_{\rm mIR}$-$\widetilde{V}$) relation of Ref. [6], the plot also deviates markedly from the proportionality with P, although it does move to lower left. The microscopic origin for these deviations is beyond the scope of this work, but it could be related to an inappropriateness of the hybridized band model at low P range, as discussed below.

As pointed out earlier, the dependence of $E_{\rm mIR}$ on $A^{-1/4}$ seems different between below and above 10 GPa. Namely, $E_{\rm mIR}$ is almost linear in $A^{-1/4}$ with different slopes between below and above 10 GPa. Since the average Yb valence in $YbCu_2Ge_2$ at low P is close to 2 (divalent), the hybridized band model may not be appropriate, which could be responsible for the deviation of $E_{\rm mIR}$ vs $A^{-1/4}$ graph from proportionality. In the photoemission spectrum

of $YbCu_2Ge_2$ at P=0 [4], a strong peak due to f^{14} (Yb^{2+}) state has been observed about 0.2 eV below E_F. Therefore, it is probably more natural to interpret the mIR peak in $\sigma(\omega)$ at low P range as arising from excitations from this f^{14} state to the unoccupied states above E_F. Then, the lower-energy shifts of mIR peak with P show that the f^{14} level is moving up toward E_F with increasing P. This is consistent with the observed increase of average Yb valence with P [2], since the f electron number should decrease as the tail of f^{14} state crosses E_F. Such an upward shifts of f^{14} level is expected by simple theoretical consideration [15], but has rarely been observed by a spectroscopic experiment. At higher P range, on the other hand, the evolutions of E_{mIR} may be more appropriately interpreted using the hybridized band model, since the f^{14} state should be actually crossing E_F. Then, the change of slope from below to above 10 GPa in Figs. 2(a) and 2(b) might correspond to the low and high P ranges in the above scenario. More detailed analyses including the T dependences of $\sigma(\omega)$ will be presented in a future publication.

4. Summary

$\sigma(\omega)$ spectra of $YbCu_2Ge_2$ at 295 K have been measured at high P to 20 GPa. A pronounced mIR peak has been observed in $\sigma(\omega)$, and has shown significant shifts to lower energy with increasing P. The P induced shifts of mIR peak has been analyzed in terms of the c-f hybridization energy, using the T^2 coefficient of $\rho(T)$. It is suggested that the P evolution of E_{mIR} at low P range corresponds to the upward shift of f^{14} state toward E_F with P, and that at high P range to the evolution of the c-f hybridized bands.

5. Acknowlegment

Experiments at SPring-8 were performed under approval by JASRI (2014B1751, 2014B1749, 2015B1698, 2015B1697). H. O. acknowledges financial support from JSPS KAKENHI (21102512, 23540409, 26400358).

References

[1] N. D. Dung, T. D. Matsuda, Y. Haga, S. Ikeda, E. Yamamoto, T. Ishikura, T. Endo, S. Tatsuoka, Y. Aoki, H. Sato, T. Takeuchi, R. Settai, H. Harima, and Y. Ōnuki, J. Phys. Soc. Jpn. **78**, 084711 (2009).
[2] A. Miyake, F. Honda, T. Watanuki, A. Machida, D. Kawana, K. Shimizu, R. Settai, and Y. Ōnuki, unpublished data.
[3] A. Miyake, F. Honda, R. Settai, K. Shimizu, and Y. Ōnuki, J. Phys. Soc. Jpn. **81**, SB054 (2012).
[4] A. Yasui, S.-I. Fujimori, I. Kawasaki, T. Okane, Y. Takeda, Y. Saitoh, H. Yamagami, A. Sekiyama, R. Settai, T. D. Matsuda, Y. Haga, and Y. Ōnuki, J. Phys.: Conf. Ser. **273**, 012067 (2011).
[5] For a recent review, see, for example, R. Y. Chen and N. L. Wang, Rep. Prog. Phys. **79**, 064502 (2016), and the references cited therein.
[6] H. Okamura, T. Watanabe, M. Matsunami, T. Nishihara, N. Tsujii, T. Ebihara, H. Sugawara, H. Sato, Y. Ōnuki, Y. Ishikawa, T. Takabatake, and T. Nanba, J. Phys. Soc. Jpn. **76**, 023703 (2007).
[7] H. Okamura, Y. Ikemoto, T. Moriwaki, and T. Nanba, Jpn. J. Appl. Phys. **56**, 05FA11 (2017).
[8] S. Kimura and H. Okamura, J. Phys. Soc. Jpn. **82**, 021004 (2013).
[9] Y. Ikemoto, T. Moriwaki, T. Hirono, S. Kimura, K. Shinoda, M. Matsunami, N. Nagai, T. Nanba, K. Kobayashi, and H. Kimura, Infrared Phys. Tech. **45**, 369 (2004).
[10] T. Moriwaki and Y. Ikemoto, Infrared Phys. Tech. **51**, 400 (2008).
[11] M. Dressel and G. Grüner, *Electrodynamics of Solids* (Cambridge University Press, Cambridge, 2002).
[12] H. Okamura, J. Phys. Conf. Ser. **359**, 012013 (2012).
[13] D. L. Cox, Phys. Rev. Lett. **58**, 2730 (1987).

[14] P. Coleman, "Heavy fermions and the Kondo lattice: a 21st century perspevtive", arXiv:1509.05769 (2015).
[15] K. Nishiyama, T. Mito, G. Pristas, T. Koyama, K. Ueda, T. Kohara, S. Gabani, K. Flachbart, H. Fukazawa, Y. Kohori, N. Takeshita, N. Shitsevalova, and H. Ikeda, Phys. Rev. B **93**, 121111(R) (2016).